Pattern Recognition, Vol. 26, No. 7, pp. 1047–1055, 1993
Printed in Great Britain

0031-3203/93 $6.00 + .00
Pergamon Press Ltd

A MODEL FOR INTERPRETING FINGERPRINT TOPOLOGY

B. G. SHERLOCK† and D. M. MONRO‡

† Department of Electrical Engineering, Parks College of Saint Louis University, Cahokia, IL 62206, U.S.A.
‡ School of Electronic and Electrical Engineering, University of Bath, Claverton Down, Bath BA2 7AY, U.K.

(*Received* 14 *July* 1992; *in revised form* 18 *December* 1992; *received for publication* 5 *January* 1993)

Abstract—A simple mathematical model is developed which computes fingerprint local ridge orientation from core and delta positions. This model provides an intelligent tool for resolving ambiguities due to the periodic nature of orientation, in algorithms for interpreting fingerprint patterns.

Direction field Fingerprint processing Ridge orientation Image analysis Mathematical model

1. INTRODUCTION

This paper describes a model of fingerprint ridge orientation. The model incorporates an understanding of the topology of fingerprints and is therefore of value in the interpretation of fingerprint images in automated fingerprint identification systems (AFIS). AFIS systems are of increasing interest and we resolve here one of the basic issues underlying fingerprint interpretation, namely that of resolving ambiguities in the recognition of ridge orientation.

In a fingerprint the ridge structure defines everywhere a direction of ridge "flow", called the local ridge orientation (LRO). Two types of singular points, cores and deltas (see Fig. 1), form isolated singularities of the otherwise continuous LRO function.

Ridge orientation has proven to be of fundamental importance in fingerprint image processing. The directional image introduced by Mehtre *et al.*[1] consists of the LRO evaluated at each pixel position in the image. Applications requiring knowledge of ridge orientation include filtering to enhance fingerprint images,[2,3] detection of singular points,[4] fingerprint image segmentation,[1,5] ridge detection during preprocessing,[6] postprocessing to reduce numbers of false minutiae[7] and pattern analysis to extract classification types.[8–11]

Several AFIS-based techniques of fingerprint enhancement and pattern analysis require (ideally) a value for fingerprint LRO at every pixel.[12] The most usual approach in commercial AFIS systems has been to determine LRO accurately on a coarse regularly spaced grid, and assume it is constant within each rectangular area. This is particularly unsatisfactory in regions near cores and deltas, where the ridge curvature is high. For example, the AFIS system developed by the U.K. Home Office[13] directionally enhances images only in low-curvature regions. By incorporating the model the enhancement can be applied to the entire image, greatly improving the encoding which follows. Another, more satisfactory, approach has been to use the directional image.[2,3] Our model is also useful here because it can guide the process of LRO determination, yielding a better quality directional image, particularly for noisier images.

Much work in the description and analysis of orientations in general images has been applied to fingerprint image processing. Kass and Witkin[14] analyze oriented patterns by estimating dominant local orientations and combining these to construct a flow coordinate system. Applied to fingerprints this approach can determine the LRO pattern and locate the singular points. Zucker[15] described orientations in terms of tangent vector fields, distinguishing between Type I (contour) and Type II (flow) processes. Fingerprint LRO is an example of a Type II process. More recently, Zucker and others have developed techniques of trace inference and curve detection[16,17] which have successfully detected ridges in fingerprints. This work, and related work for 3-dimensional images[18,19] is of interest because it applies differential geometric concepts such as tangent fields, direction fields and Poincare indices to the analysis of image directionality. It is not, however, immediately applicable to the problem of modeling LRO because LRO represents a flow-like (2-dimensional) rather than a curve-like (1-dimensional) process. Fingerprint pattern classification techniques in the literature[8–10] often depend upon an analysis of the LRO pattern. While this paper does not directly address the classification problem, our model has an understanding of LRO topology and can therefore be usefully applied to pattern classification.

As mentioned above, many applications must process ridge orientation information. Ambiguities due to the multi-valued nature of orientation modulo π can occur during the analysis of the LRO pattern. Without an intelligent model which understands the topological behavior of ridge orientation, it is difficult to resolve these ambiguities satisfactorily. Section 3 concerns the nature of the ambiguities and the use of the model to resolve them. The result is demonstrated in an algorithm for interpolating between sampled values of LRO.

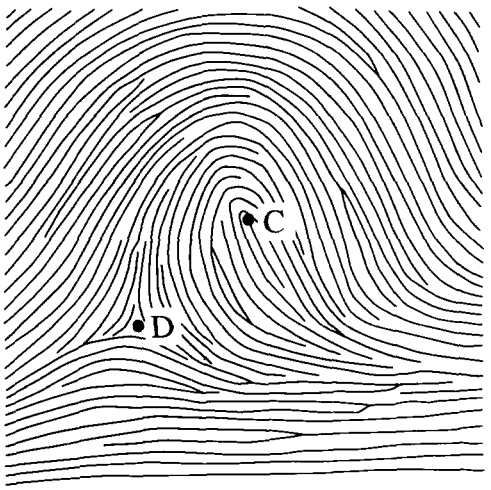

Fig. 1. A loop fingerprint, showing two singular points, marked C at the core and D at the delta.

2. THE MODEL OF RIDGE ORIENTATION TOPOLOGY

2.1. *Direction and orientation*

Two distinct types of direction can be defined. One of these, which we shall call simply "direction", is easily described by the elementary mathematics of vectors. The other, called "orientation", is more useful for describing directionality in images, but requires the concept of the "direction field". We adopt the term direction field from differential geometry[20] even though "orientation field" might be a less confusing description in view of our distinction between direction and orientation.

As we shall see, the direction field is suitable for describing the behavior of fingerprint ridge orientation in the vicinity of cores and deltas, whereas the vector field is not.

A vector in the plane, as shown in Fig. 2(a), forms some angle θ with the Cartesian x-axis. θ is in the range 0 to 2π rad and is called the *direction* of the vector. Directions of vectors can be naturally represented as elements of the unit circle S^1. Since we will be interested only in the directional properties of vectors, all vectors will be assumed to have unit length.

Figure 2(b) shows a straight line through the origin instead of a vector. This line forms some small positive angle θ with the positive x-axis. θ is called the *orientation* of the line and lies in the range 0 to π because it is unaffected by rotation through integer multiples of π. Orientations can be represented as elements of the projective circle P^1 which may be thought of as a circle with circumference π and radius 1/2. (Mathematically, the *projective n-space* P^n is obtained by identifying radially opposite points of the unit n-sphere S^n.)

2.2. *Vector fields and direction fields*

A vector field can be regarded as a 2D function assigning a direction in S^1 to each point. Analogously, a *direction field*[21] can be regarded as a 2D function taking on values which are orientations in P^1. In both

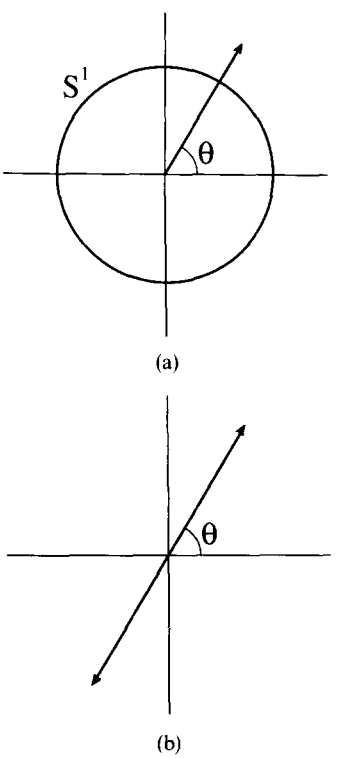

Fig. 2. Illustrating the difference between (a) direction and (b) orientation.

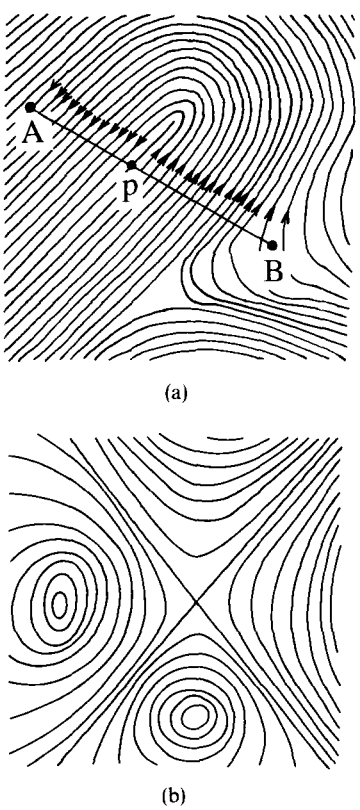

Fig. 3. Two sets of curves. The curves in (b) are orientable; those in (a) are not.

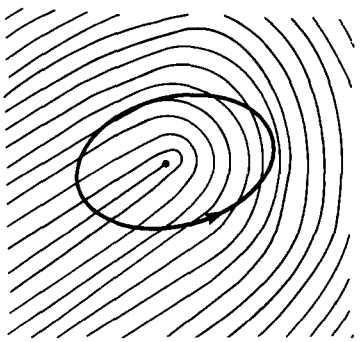

(a)

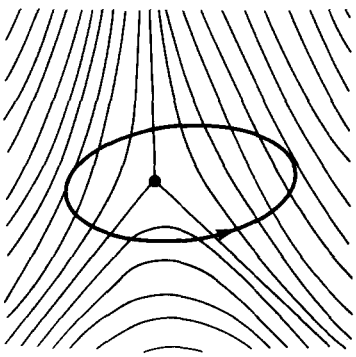

(b)

Fig. 4. Poincare indices for direction field singular points: (a) core (index 1/2); (b) delta (index $-1/2$).

cases the function is defined and continuous everywhere except at a finite number of *singular points*.

The fundamental difference between vector and direction fields is revealed when their integral curves are compared. An *integral curve* of the field is a curve whose tangent has everywhere the same direction (or orientation) as the field. Integral curves of vector fields are always orientable; that is, it is possible to assign arrows to the curves, indicating a forward sense of "flow" which is consistent and continuous. However, direction fields need not be orientable. Figure 3 shows examples of orientable and non-orientable sets of curves. In the non-orientable example, a discontinuous change in the sense of the arrows occurs at the point p along the path AB shown.

It is in the concept of orientability that we find a vector field unsuitable to model realistic fingerprints, and a direction field suitable. Note the similarity between the non-orientable example of Fig. 3 and the ridge pattern of a loop fingerprint.

The difference between direction and vector fields is also revealed by the Poincare indices[21] of the singular points of the field. The Poincare index of a singular point p is the net or algebraic number of rotations through 2π made by the direction (or orientation) of the field as a simple closed curve surrounding p and no other singular point is traversed in the anticlockwise sense. It is well known that Poincare indices in vector fields are always integers. For direction fields the indices may also be half-integers.[22] Figure 4 shows patterns of lines resembling the areas around cores and deltas in fingerprints, showing that the index of a core is $+1/2$ and the index of a delta is $-1/2$, corresponding to changes in LRO of π and $-\pi$, respectively, as the curve is traversed. The center of a circular whorl has an index of $+1$ and can be regarded as two superimposed cores. The values of Poincare indices for the various LRO singularities were noted in reference (11). Sander and Zucker[18] have described these singularity types, their Poincare indices, and the use of direction fields to describe surfaces in 3D images.

Our use of the direction field provides a mathematical basis for describing fingerprints. Without it the orientation of ridges could not have been modeled in a manner which exhibits the non-orientability and Poincare index values characteristic of fingerprints.

2.3. *A model of LRO topology*

It should now be clear that a local ridge orientation function LRO(x, y) can be modeled as a direction field having singular points $d_1 \cdots d_m$ of index $-1/2$ at delta points and $c_1 \cdots c_k$ of index $1/2$ at core points.

The model of LRO which is developed here is the simplest possible model which accounts correctly for the topological behavior of orientation around the singular points. It provides a direction field $\theta(x, y)$ which is deformable onto the true LRO field of a real fingerprint. Any two fingerprints with the same singular points are modeled by the same function, even though their LRO values may differ in detail. Each pattern can, however, be continuously mapped onto the other. Therefore, the $\theta(x, y)$ of the model can be regarded as the LRO of some "ideal" fingerprint having the given core and delta positions. Its relation to the actual LRO of a real fingerprint is discussed in the next section and its usefulness in real applications is described in the sections which follow.

We now describe the model. First, regarding the image plane as the complex plane C, consider the rational polynomial function

$$q(z) = \frac{(z - z_1)(z - z_2)\cdots(z - z_k)}{(z - p_1)(z - p_2)\cdots(z - p_m)}$$

with first-order poles and zeros $p_1, \ldots, p_m$ and $z_1, \ldots, z_k$. It is well known that the Poincare indices are $+1$ at each zero and -1 at each pole.

We observe empirically that far from the center of the image, the ridge orientation tends towards a constant value, say θ_∞. Noting that the cores and deltas of a fingerprint have Poincare indices of $1/2$ and $-1/2$, define

$$p(z) = \sqrt{\left(e^{2j\theta_\infty} \cdot \frac{(z - z_{c1})(z - z_{c2})\cdots(z - z_{cm})}{(z - z_{d1})(z - z_{d2})\cdots(z - z_{dm})} \right)}$$

where $z_{c1}, \ldots, z_{ck}$ and $z_{d1}, \ldots, z_{dk}$ are the locations of the cores and deltas, respectively, and θ_∞ is the ridge slope at infinity. With the usual alignment, $\theta_\infty = 0$.

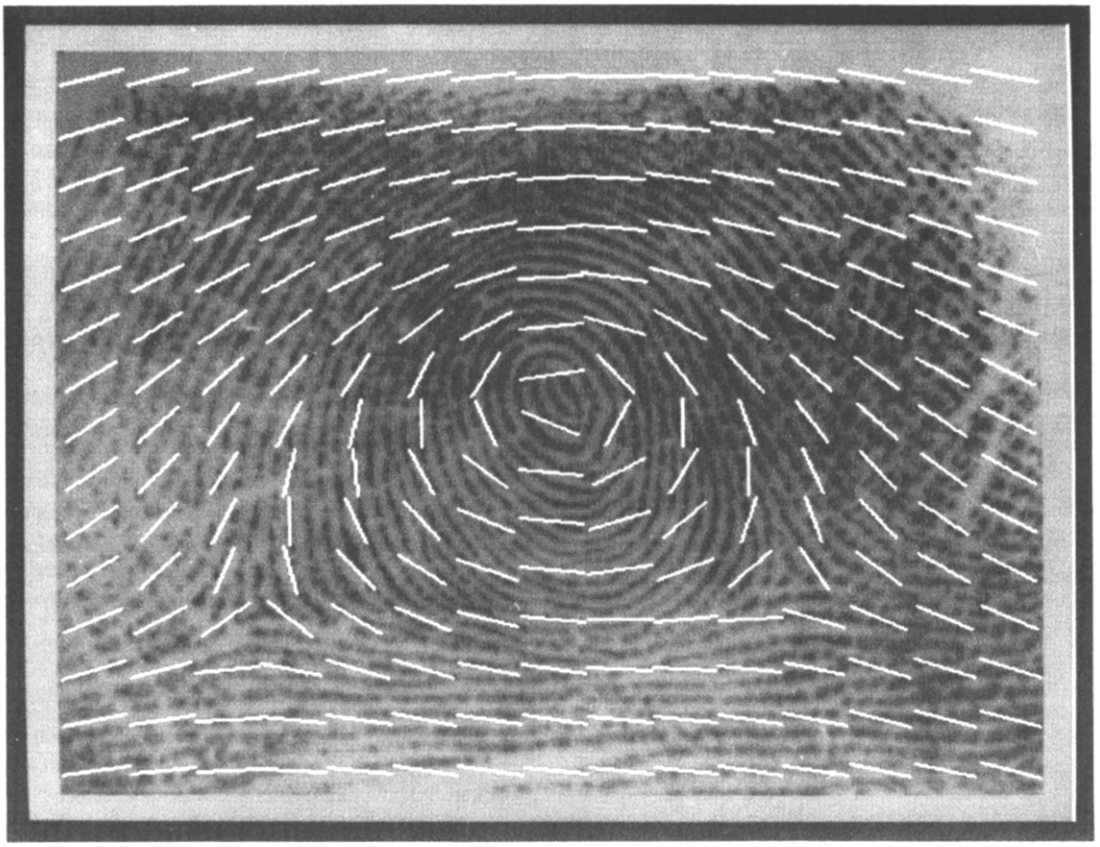

(a)

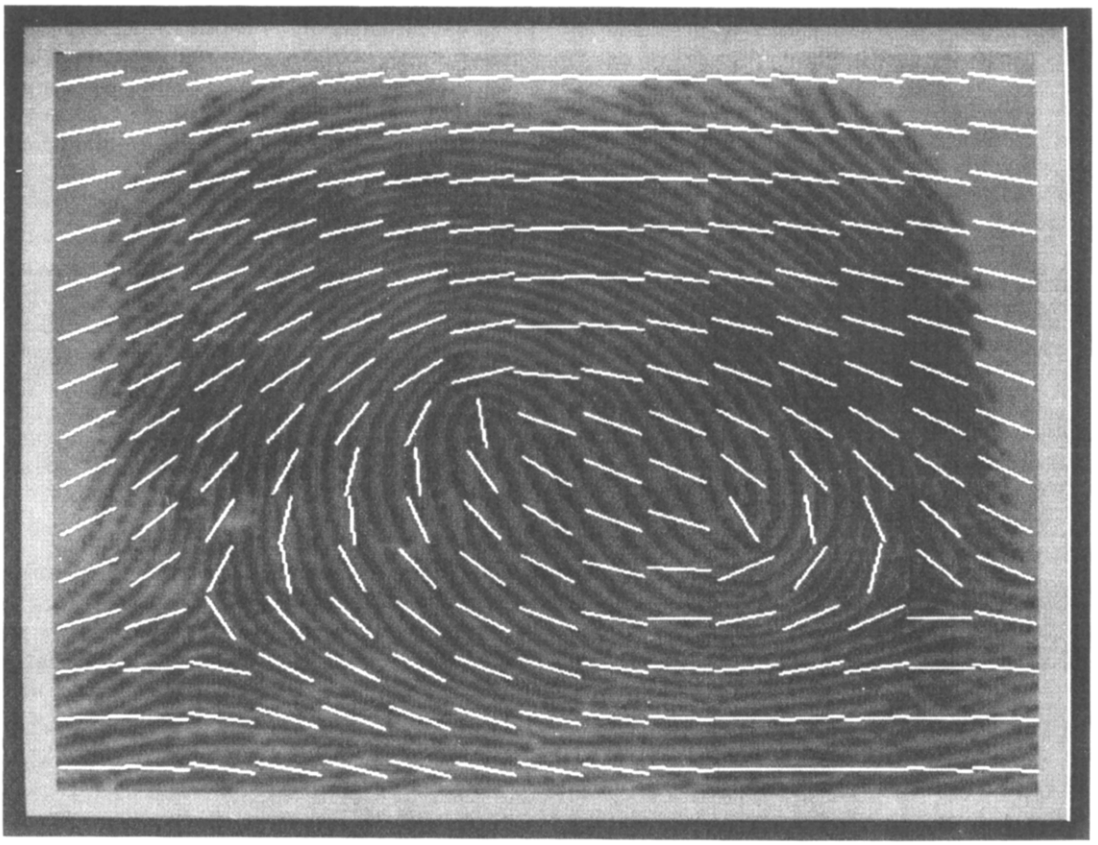

(b)

Fig. 5. LRO patterns determined by the model: (a) whorl; (b) double loop; (c) loop; (d) tented arch; (e) plain arch.

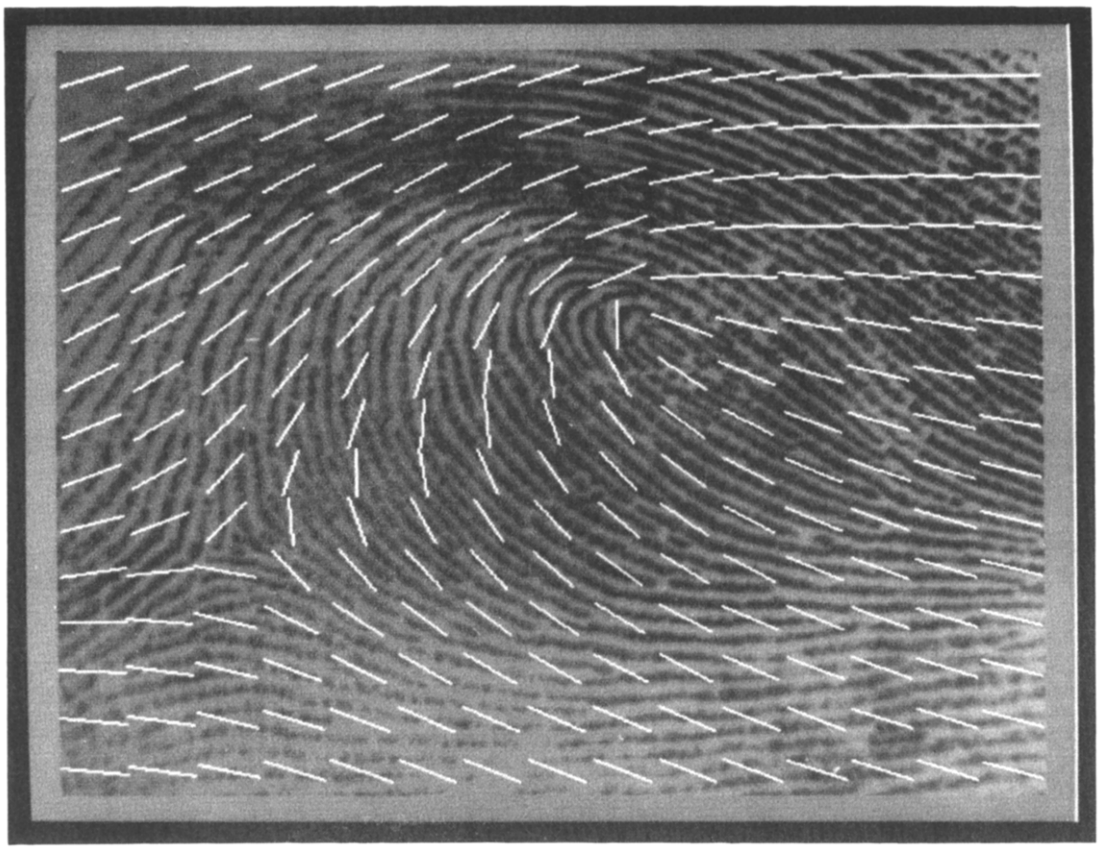

(c)

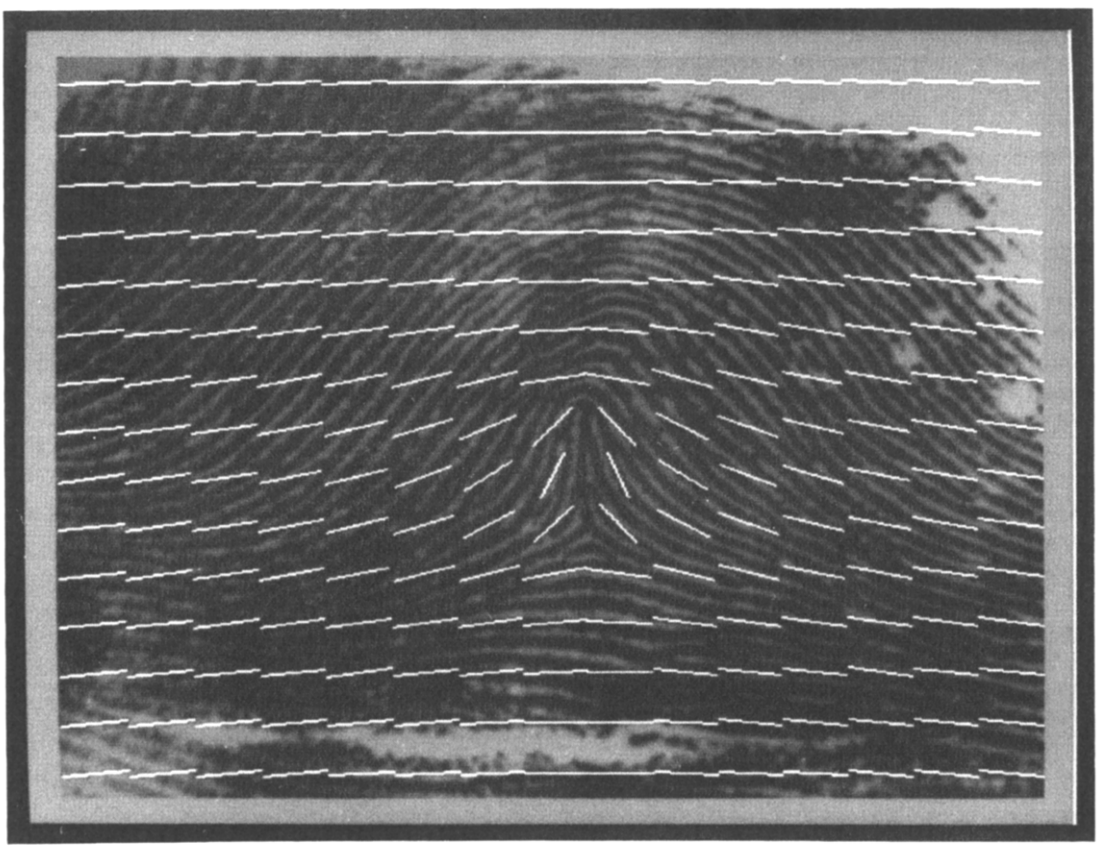

(d)

Fig. 5. (*Continued.*)

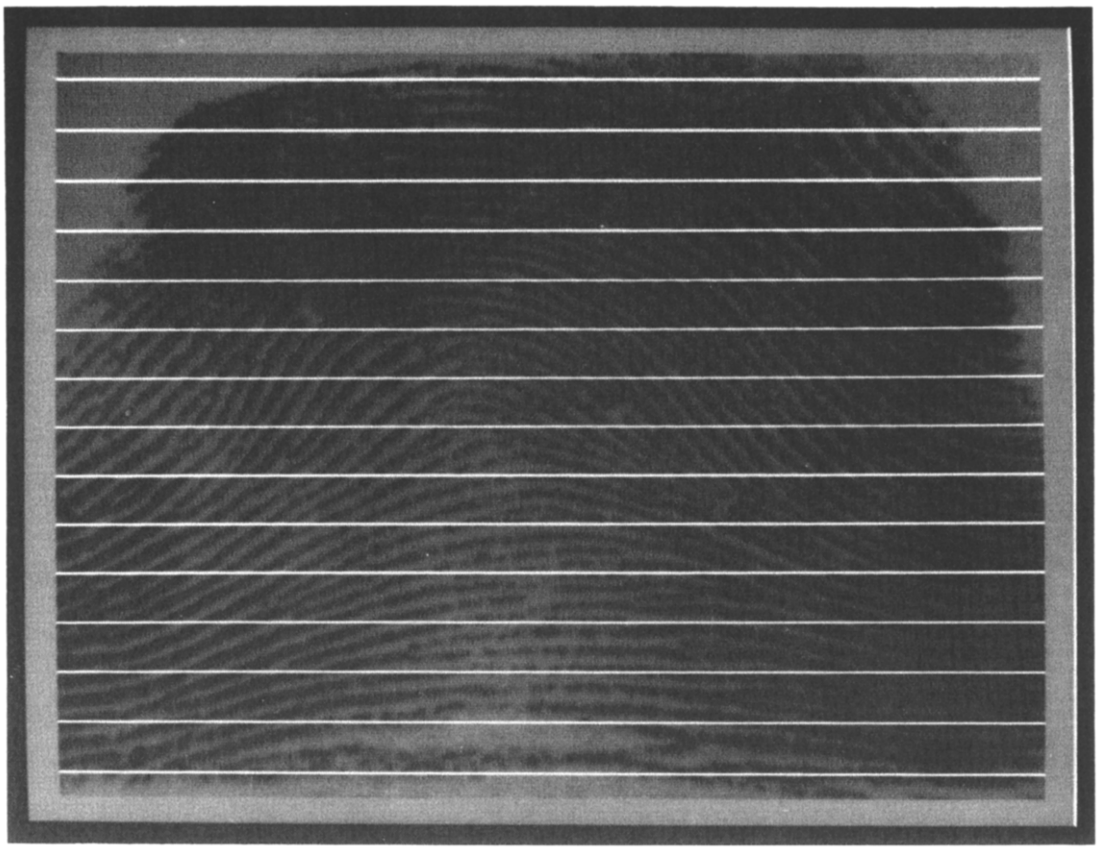

(e)

Fig. 5. (*Continued.*)

The above equation has the required half-integral Poincare indices, since taking the square root of a complex number halves its argument.

Thus the model of LRO is

$$\theta(z) = (\arg(p(z))) \bmod \pi.$$

2.4. *Relationship to the LRO of real fingerprints*

The actual LRO of a real fingerprint is a direction field with singular points at the cores and deltas. The modeled orientation $\theta(x, y)$ is a direction field with identical singular point positions and types. Therefore, $\mathrm{LRO}(x, y) = \theta(x, y) + \varepsilon(x, y)$ where the error $\varepsilon(x, y)$ is a direction field having indices of value zero at all singular points.

Figure 5 shows fingerprints of the plain arch, tented arch, whorl, loop and double loop classification types. Line segments representing orientations determined by the model are superimposed. The model correctly represents the topological behavior of the ridge structure, but does not provide close point-wise approximation to the true values. Therefore, the usefulness of the model lies not in providing accurate orientation values but in providing knowledge about their behavior.

3. USE OF THE MODEL TO RESOLVE AMBIGUITIES IN LRO

Applications requiring knowledge of ridge orientation include filtering to enhance fingerprint images and pattern analysis to extract classification types and minute details in AFIS systems.

Traditional methods of real analysis assume that the function being analyzed is continuous and real-valued. Problems arise when processing orientations because this basic assumption is violated. Although LRO is continuous as a function taking values in P^1, it is usually discontinuous (and indeed multi-valued) when viewed as real-valued.

The multi-valued nature of orientation leads to ambiguities when processing orientations. Suppose for

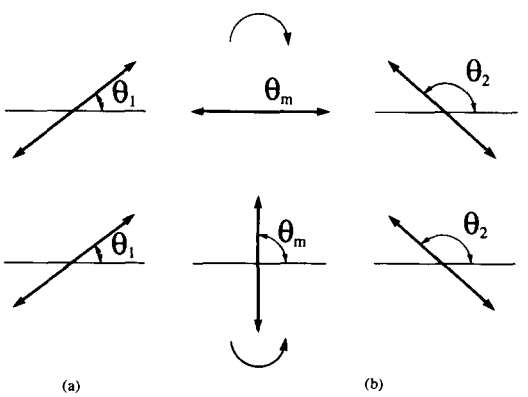

Fig. 6. Two orientations $\theta_1 = \pi/4$ and $\theta_2 = 3\pi/4$, with the interpolated midpoint values θ_m: (a) $\theta_m = 0$ obtained assuming clockwise rotation from θ_1 to θ_2; (b) $\theta_m = \pi/2$ obtained assuming anticlockwise rotation.

example that interpolated orientation values are required along the line joining points p_1 and p_2, where $\theta(p_1) = 3\pi/4$ and $\theta(p_2) = \pi/4$ (say) as in Fig. 6. There are infinitely many ways of reaching $3\pi/4$ from $\pi/4 - P^1$ may be circumnavigated any number of times in either sense. The figure shows two of these options, which yield different results.

If the rate of change of θ is known, the ambiguity is resolved. The sign of the derivative indicates whether to move clockwise or anticlockwise around P^1, and its magnitude indicates the number of revolutions required. With a suitable sampling rate, the number of full revolutions is always zero, and the choice is simply between clockwise and anticlockwise rotation. The LRO model provides the information required to make this choice.

3.1. *Orientation unwrapping*

Standard 2D analysis could be applied to LRO if it were possible to "unwrap" $\theta(x, y)$, converting it into a continuous real-valued function $\theta_u(x, y)$. Unwrapping is performed by adding a suitable multiple of π to each sample, thereby removing the discontinuities. Unfortunately, the following result applies.

Theorem. A 2D orientation valued function $\theta(x, y)$ cannot be unwrapped if it has a singular point.

Proof. Let p be singular. Assume θ can be unwrapped, yielding θ_u. Let C be a simple closed curve around p, and (x, y) any point on C. As C is traversed anticlockwise from (x, y), θ_u changes through $2\pi \cdot \mathrm{i}x(p)$ to its final value $\theta_u(x, y) + 2\pi \cdot \mathrm{i}x(p)$. This final value occurs at the same point (x, y), so by continuity of θ_u, $\theta_u(x, y) = \theta_u(x, y) + 2\pi \cdot \mathrm{i}x(p)$. So $\mathrm{i}x(p) = 0$, contradicting the statement that p is singular. Q.E.D.

However, unwrapping is always possible in the 1D case. For each x in increasing order, choose an integer $k(x)$ which makes $\theta_u(x) = \theta(x) + k(x)\pi$ continuous from 0 to x. Figure 7 shows an orientation function and its unwrapped version.

Phase unwrapping[23,24] is a related problem where the phase $\theta(\omega)$ of the Discrete Fourier Transform of some signal $f(x)$ must be unwrapped. The unwrapped phase takes the form $\theta_u(\omega) = \theta(\omega) + k(\omega) \cdot 2\pi$ where k is integral. Solutions to this problem find $k(\omega)$ by using the signal data $f(x)$ to estimate the phase derivative $\theta'(\omega)$. Phase unwrapping does not apply directly to orientation unwrapping because there is no corresponding signal. However, the same general approach can be applied by using the LRO model to estimate the derivative of the orientation.

The ability to unwrap 1D functions permits a restricted form of analysis of orientations in two dimensions. Given a simple curve $C(t)$ not passing through singularities of $\theta(x, y)$, the 1D function $\theta(C(t))$ can be unwrapped along the curve yielding $\theta_u(C(t))$. Ordinary analysis can then be applied along C using any classical algorithm. In particular, C could be any straight line parallel to either coordinate axis, and the entire image can be covered by such lines.

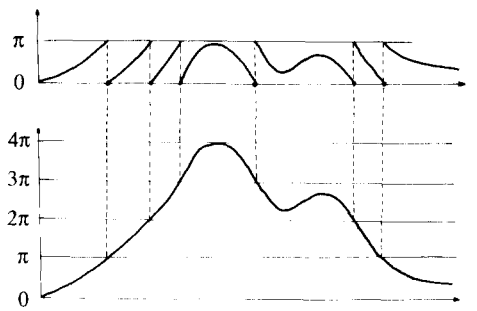

Fig. 7. A 1D orientation function (above) and its unwrapped version (below).

3.2. *Use of the LRO model for orientation unwrapping*

An estimate of the derivative of the orientation is given by the gradient of the modeled LRO function:

$$\nabla\theta = \nabla(\arg p(z)) = \frac{1}{2}\sum_{i=1}^{k}\left\{\frac{(y_{ci}-y, x-x_{ci})}{(x-x_{ci})^2+(y-y_{ci})^2} - \frac{(y_{di}-y, x-x_{di})}{(x-x_{di})^2+(y-y_{di})^2}\right\}.$$

With an appropriate sampling rate, LRO changes by less than π rad between samples. If so, only the sign of the derivative is required. With this simplification, the unwrapping algorithm is:

```
procedure unwrap(var x, xdot: array of real)
{x is the data to be unwrapped, and   }
{xdot is the array of derivative values   }
const
  maxdiff = π/4
begin
  x[1]:=x[1] mod π
  for i:=2 to length of x do
    Restrict x[i] to the range x[i − 1] − π/2..x[i − 1]
    + π/2 by adding or subtracting a suitable multiple
    of π.
    diff:=x[i] − x[i − 1]
    if (diff > maxdiff) and (xdot[i] < 0) then
      x[i]:=x[i] − π
    elseif (diff < −maxdiff) and (xdot[i] > 0) then
      x[i]:=x[i] + π
    endif
  endfor
end
```

3.3. *Application to interpolation of orientations*

Since determining ridge orientation reliably can be computationally demanding unless special hardware is available, it is often not feasible to evaluate LRO directly for each pixel. Our approach is to determine

the LRO at a square grid spaced (say) 16 pixels apart, and obtain intermediate values by interpolation.† During interpolation, the multi-valued nature of orientation leads to ambiguities which can be resolved by the model as described earlier. The algorithm for interpolating an n by n array of orientations by a factor K is

```
{We have n rows and n columns of data}
for i:=1 to n do
   unwrap row i
   interpolate row i by factor K
endfor

{We now have n rows and n*K columns}
for i:=1 to n*K do
   unwrap column i
   interpolate column i by factor K
   wrap column i
endfor
{We now have n*K rows and n*K columns}
```

Provided that the unwrapping does not fail, the behavior of the above interpolation algorithm is identical to that of the standard interpolation technique incorporated within it.

4. CONCLUSION

This paper has shown that fingerprint local ridge orientation can be best described using the direction field concept of differential geometry, rather than the more usually encountered vector field. A simple model of fingerprint local ridge orientation topology in terms of the positions of cores and deltas has been presented, and shown to be of practical use in the 2D interpolation of sampled LRO values from real fingerprints. The model emphasizes the fundamental importance of core and delta numbers and positions in determining the topology of the fingerprint LRO structure.

REFERENCES

1. B. M. Mehtre *et al.*, Segmentation of fingerprint images using the directional image, *Pattern Recognition* **20**, 429–435 (1987).
2. L. O'Gorman and J. V. Nickerson, An approach to fingerprint filter design, *Pattern Recognition* **22**, 29–38 (1989).
3. L. O'Gorman and J. V. Nickerson, Matched filter design for fingerprint image enhancement, *Inf. Conf. Acoustics, Speech, Signal Processing*, New York, pp. 916–919 (1988).
4. V. S. Srinivasan and N. N. Murthy, Detection of singular points in fingerprint images, *Pattern Recognition* **25**, 139–153 (1992).
5. B. M. Mehtre and B. Chatterjee, Segmentation of fingerprint images—a composite method, *Pattern Recognition* **22**, 381–385 (1989).
6. M. R. Verma *et al.*, Edge detection in fingerprints, *Pattern Recognition* **20**, 513–523 (1987).
7. Q. Xiao and H. Raafat, Fingerprint image postprocessing: a combined statistical and structural approach, *Pattern Recognition* **24**, 985–992 (1991).
8. C. V. K. Rao and K. Balck, Type classification of fingerprints: a syntactic approach, *IEEE Trans. Pattern Analysis Mach. Intell.* **PAMI-2**, 223–231 (1980).
9. A. Grasselli, On the automatic classification of fingerprints, *Methodologies of Pattern Recognition*, S. Watanabe, ed. Academic Press, New York (1969).
10. B. Moayer and K. S. Fu, A syntactic approach to fingerprint pattern recognition, *Pattern Recognition* **7**, 1–23 (1975).
11. M. Kawagoe and A. Tojo, Fingerprint pattern classification, *Pattern Recognition* **17**, 295–303 (1984).
12. J. P. Riganati, An overview of algorithms employed in automated fingerprint processing, *Proc. Int. Conf. on Crime Countermeasures*, Lexington, Kentucky, pp. 125–131 (1977).
13. K. Millard, Developments on automatic fingerprint recognition, *Int. Carnahan Conf. on Security Technology*, Zurich, pp. 173–178 (1983).
14. M. Kass and A. Witkin, Analyzing oriented patterns, *Comput. Vision Graphics Image Process.* **37**, 362–385 (1987).
15. S. W. Zucker, Early orientation selection: tangent fields and the dimensionality of their support, *Comput. Vision Graphics Image Process.* **32**, 74–103 (1985).
16. C. David and S. W. Zucker, Potentials, valleys, and dynamic global coverings, *Int. J. Comput. Vision* **5**, 219–238 (1990).
17. P. Parent and S. W. Zucker, Trace inference, curvature consistency, and curve detection, *IEEE Trans. Acoustics Speech Signal Process.* **11**, 823–839 (1989).
18. P. T. Sander and S. W. Zucker, Singularities of principle direction fields from 3-D images, *IEEE Trans. Pattern Analysis Mach. Intell.* **14**, 309–317 (1992).
19. P. T. Sander and S. W. Zucker, Inferring surface trace and differential structure from 3-D images, *IEEE Trans. Pattern Analysis Mach. Intell.* **12**, 833–854 (1990).
20. M. Spivak, *A Comprehensive Introduction to Differential Geometry*, Vol. I. Publish or Perish, Berkeley (1979).
21. C. Godbillon, *Dynamical Systems on Surfaces*. Springer, Berlin (1983).
22. M. Spivak, Singularities of line fields, *A Comprehensive Introduction to Differential Geometry*, Vol. III, Chapter 4, Addendum 2. Publish or Perish, Berkeley (1979).
23. A. V. Oppenheim and R. W. Schafer, *Digital Signal Processing*. Prentice-Hall, Englewood Cliffs, New Jersey (1975).
24. J. M. Tribolet, A new phase unwrapping algorithm, *IEEE Trans. Acoustics Speech Signal Process.* **ASSP-25**, 170 (1977).

† An alternative, equally acceptable approach is to use a faster-running but perhaps less reliable algorithm to estimate orientation at every pixel position, and to smooth the resultant orientation image.[2,3]

About the Author—B. G. SHERLOCK received the B.Sc. (1979) and M.Sc. (1983) degrees in electrical engineering at the University of Cape Town, and the Ph.D. (1989) degree from Imperial College, London. After two years with De La Rue Printrak Ltd, Basingstoke, U.K., he took up his present position as Assistant Professor in the Electrical Engineering Department at Parks College of Saint Louis University. His research interests are in signal and image processing and modeling and simulation of electronic devices.

About the Author—D. M. MONRO is Professor of Electronics at the University of Bath in south west England. Of Canadian origin, he received the BASc (1964) and MASc (1966) degrees from the University of Toronto and spent a short time in the aeronautical industry before studying for the Ph.D. degree at Imperial College, London which was awarded in 1971. He held academic posts in electrical engineering and computing at Imperial College before taking up his present position in 1991. His research interests are in image processing, parallel computers, and modeling electromagnetic fields in biological tissue.